Characterization and evolution of the *Swift* X-ray Telescope instrumental background

C. Pagani*[a], D. C. Morris[a], J. Racusin[a], D. Grupe[a], L. Vetere[a], M. Stroh[a], A. Falcone[a], J. A. Kennea[a], D. N. Burrows[a], J. A. Nousek[a], A. F.Abbey[b], L. Angelini[c], A. P. Beardmore[b], S. Campana[d], M. Capalbi[e], G. Chincarini[d], O. Citterio[d], G. Cusumano[f], P. Giommi[e], O. Godet[b], J. E. Hill[g,h], V. LaParola[f], V. Mangano[f], T. Mineo[f], A. Moretti[d], J. P. Osborne[b], K. L. Page[b], M. Perri[e], P. Romano[d], G. Tagliaferri[d], F. Tamburelli[e]

[a]Pennsylvania State University, 525 Davey Lab, Univesity Park, PA 16802, USA;
[b]University of Leicester, University Road, Leicester, LE1 7RH, UK;
[c]NASA-GSFC, Greenbelt, MD 20711, USA;
[d]INAF-Osservatorio Astronomico di Brera, Via E. Bianchi 46, 23807, Merate, LC, Italy;
[e]ASI-ASDC, Via G. Galilei, I-00044 Frascati, Italy;
[f]INAF-IASF, Via U. La Malfa 153, 90146 Palermo, Italy;
[g]Universities Space Research Association, 10211 Wincopin Circle, Suite 500, Columbia, MD 21044, USA;
[h]CRESST and NASA Goddard Space Flight Center, Greenbelt, MD 20771, USA

ABSTRACT

The X-ray telescope (XRT) on board the *Swift* Gamma Ray Burst Explorer has successfully operated since the spacecraft launch on 20 November 2004, automatically locating GRB afterglows, measuring their spectra and lightcurves and performing observations of high-energy sources. In this work we investigate the properties of the instrumental background, focusing on its dynamic behavior on both long and short timescales. The operational temperature of the CCD is the main factor that influences the XRT background level. After the failure of the *Swift* active on-board temperature control system, the XRT detector now operates at a temperature range between -75C and -45C thanks to a passive cooling Heat Rejection System. We report on the long-term effects on the background caused by radiation, consisting mainly of proton irradiation in *Swift*'s low Earth orbit and on the short-term effects of transits through the South Atlantic Anomaly (SAA), which expose the detector to periods of intense proton flux. We have determined the fraction of the detector background that is due to the internal, instrumental background and the part that is due to unresolved astrophysical sources (the cosmic X-ray background) by investigating the degree of vignetting of the measured background and comparing it to the expected value from calibration data.

Keywords: *Swift*, X-ray telescope, CCD detector, X-rays, background.

1. INTRODUCTION

The primary scientific purpose of the XRT[1] is to provide autonomous localization and to measure the flux and the spectrum of X-ray afterglows of Gamma-ray Bursts (GRBs) discovered by the Burst Alert Telescope[2] on board the *Swift*[3] spacecraft. The XRT has also performed successful observations and monitoring campaigns of high-energy astronomical sources such as X-ray transients, supernovae and Active Galactic Nuclei (see, for instance, refs[4-5-6]). The XRT uses a grazing incidence 3.5 m focal length Wolter I mirror[7] to collect X-ray photons on a e2v-22 CCD[8] designed for the EPIC MOS instruments on XMM. The Focal Plane Camera Assembly, based on the XMM/EPIC cryostat design, provides a vacuum enclosure for the detector and optical blocking for the CCD against optical light and cosmic rays. The CCD has a 0.2 to 10 keV bandpass and the image section is a 600 x 602 array of 40 μm x 40 μm pixels, each pixel corresponding to 2.36 arcseconds in the *Swift* focal plane.

*pagani@astro.psu.edu; phone 1 814 865-0233

UV, X-Ray, and Gamma-Ray Space Instrumentation for Astronomy XV, edited by Oswald H. W. Siegmund
Proc. of SPIE Vol. 6686, 668609, (2007) · 0277-786X/07/$18 · doi: 10.1117/12.734398

The instrument background at the lower end of the spectrum consists of the CCD noise due to "bad pixels" producing leakage current while at higher energies the background is caused by events generated by charged particles (cosmic rays).

On short timescales, the instrument background is strongly dependent on the CCD temperature, with the number of "hot pixels" (consistently bad pixels) and "flickering pixels" (pixels with an unstable level of dark current) increasing dramatically at temperatures above -52C. On long timescales the main cause of degradation of the CCD performance is proton irradiation. To minimize the dark current and the effects of damages caused by radiation, the original thermal design of the XRT called for a Thermo Electric Cooler (TEC) to provide active cooling to keep the detector at -100C. The failure of the TEC power supply during the early phase of the mission did not affect the scientific performance of the XRT but caused a higher level of dark current and CCD noise, because it forced the instrument to rely on the passive cooling provided by the radiator. A second major cause of increase in the CCD background has been the micrometeoroid impact[9-10] on May of 2005 that caused the appearance of new hot pixels and hot columns that are now masked on board.

A detailed knowledge of the instrumental background, its spatial variation and its dynamical behavior can be very important in various kinds of scientific analysis. In the study of the unresolved component of the cosmic X-ray background, for example, deep exposures are required and the instrument background dominates the observations. Also, when analyzing extended sources like supernova remnants, the detailed spatial dependences of the instrument background can be of primary importance, but a direct measurement of the background is not possible because the emission from such a source is spread over a large fraction of the field of view.

While the background dependence on the CCD temperature is well known[11], in this work we present our analysis on the evolution of the XRT background due to proton irradiation. We investigate the evolution of the count rate and the spectrum of the background at a range of temperatures since the beginning of the mission. *Swift* spends approximately 15% of each day in orbit transiting through the South Atlantic Anomaly (SAA), where the Earth's magnetic field is less effective in shielding the spacecraft from high-energy particles and no scientific data are taken by the XRT. We analyze the short-term effects of the SAA passages on the CCD response, monitoring the background count rate at specific time intervals after the SAA exit. We study the degree of vignetting of the XRT background to estimate, at several CCD temperatures, what fraction of events has an instrumental origin and what fraction comes from unresolved astrophysical sources, i.e., the cosmic X-ray background.

2. ANALYSIS STRATEGY

The study of the XRT instrumental background is complicated by the fact that there is no "closed door" configuration that could be used for observations to exclude photons from the cosmic X-ray background. However, there is a small area in each of the four corners of the CCD that is outside the XRT Field of View (FoV, defined by the frame of the circular UV/optical filter mounted on top of the lower proton shield) and therefore can be used to measure the pure internal background. Parts of this area outside the FoV have to be excluded because they are illuminated by four circular ^{55}Fe sources that are used as in-flight calibrators of the gain and charge transfer efficiency of the detector. The area of pure instrumental background is further reduced due to the fact that events collected at the edge of the CCD are not transmitted to the ground to decrease the spacecraft data volume to satisfy *Swift*'s telemetry requirements. The combination of the small area and the low level of the CCD background requires that a large number of observations with long exposures be analyzed to collect a statistically significant number of events to properly characterize the detector background. For this purpose, we selected every observation in the *Swift* HEASARC archive since January 2005 with an exposure time in Photon Counting (PC) mode[12] greater than 10 ks, for a total of 39 Ms of collecting time.

2.1 Long-term background evolution

The XRT background varies by more than a factor of 10 from the coldest temperature of T=-75C that has been achieved by the passive cooling to the highest temperatures at which XRT can collect scientifically useful data, T=-50C. To evaluate the evolution of the background over the first two years of the mission, we divided the observations into three

temperature ranges: *COLD*, at T<-60C; *MEDIUM*, at -60C<T<-55C; and *HOT*, T>-55C. We excluded the region inside the FoV and the corner source regions using XSELECT (v2.4), and we extracted event files both without applying any event grade selection and applying the standard 0 to 12 grade selection characteristic of real X-ray events. We excluded hot pixels in the images and to achieve a good level of statistics we merged the events from each month since 2005 using the FTOOL "*fmerge*". Finally, we extracted spectra for all grades and for grades 0 to 12.

2.2 Background variation after SAA passes

The XRT does not collect data during the SAA passes, which can last up to 30 minutes. During these passes, the instrument is exposed to a large dose of high energy particles because of the reduced natural protection of the Earth's magnetic field. The proton irradiation while in the SAA causes known long term damage to the detector by creating electron traps in the silicon lattice. In this work we investigated possible short term effects on the background due to the SAA passes, as activation of CCD cells by high energy particles, by monitoring the background count rate and spectrum.

For this study we used the same dataset of observations described previously, selecting the area of the CCD with pure instrumental background. We used the housekeeping telemetry files associated with each observation to obtain the times of the end of the SAA passes and for each dataset we calculated the difference between the arrival time of the background events and the time of the end of the SAA pass. We extracted event files using XSELECT containing events collected at increasing time intervals after a SAA pass (within 1 minute, from 1 to 5, 5 to 10 and 10 to 15 minutes after the SAA). In a few cases, artificially bright rows were present in the final images of the processed observations. These artifacts are caused by an incorrect bias subtraction due to cosmic rays strikes in a section of the CCD used for bias evaluation. We excluded the times during which the hot rows appeared and removed any remaining hot pixels from the final event files. Results are reported in Section 3.2.

2.3 Vignetting

The vignetting effect is caused by the reduced reflection efficiency and lower geometric collecting area for X-ray photons that are offset from the optical axis of the telescope. Since vignetting will only affect photons, which pass through the XRT optics, we can use knowledge of the functional form of the vignetting to distinguish between the cosmic background emission and the non-focused sources of background such as instrumental noise and high-energy particles.

The XRT vignetting (V) can be modeled as a function of distance from the center of the chip as:

$$V=1-c*\Theta^2 \quad (1)$$

where Θ is the offset in arcminutes from the center of the chip and c is a function of the energy *E* of the events of the form:

$$c=A0*A1^E+A2 \quad (2)$$

where A0=0.000124799, A1=1.55219, A2=0.00185628[13].

For our analysis we used the dataset previously described, but selecting data from 2006 only to avoid discrepancies in the number of bad columns within the dataset, since the number of bad columns has increased due to a micrometeoroid impact in May 2005. The data have been processed with the XRTPIPELINE task (XRT software version 2.2, developed at the ASI Science Data Center) with the standard input parameters and have been corrected for varying exposures to the sky and hot columns masked onboard by application of an exposure map.

We removed point sources in the images identified with XIMAGE *detect*, creating region files centered at the source positions with radii that are a function of the source luminosity and then excluding the regions using XSELECT. We omitted observations of known extended sources like supernova remnants that would not be picked up by the XIMAGE detection algorithm. We also excluded observations that were affected by Earth limb contamination: during *Swift* observations, if the Earth elevation angle (defined as the angle between the Earth limb and the *Swift* pointing direction) decreases, the XRT images can be contaminated by light from the bright Earth. The bright Earth events are not uniformly distributed over the CCD surface and would compromise measurement of the vignetting. The increase in the count rate due to the Earth Limb causes at first the XRT to autonomously switch readout mode between Photon Counting (PC) and Windowed Timing (WT) mode (the set point for the transition between PC and WT mode is currently set at 10 counts/s). As the Earth Limb optical contamination flux increases the XRT continues the observations in WT

mode. To avoid Earth Limb contamination in our dataset we excluded PC observations taken within 10 minutes of the readout mode switch times.

We, once again, divided the dataset into three temperature ranges (*COLD*, *MEDIUM* and *HOT*) as defined in the previous analysis. Finally, we merged the observations, obtaining one background event file for each of the specified temperature ranges. For each data file we evaluated the number of background events per pixel as a function of radius, from the center to the edge of the chip.

3. RESULTS

3.1 Long-term background evolution

The evolution of the XRT instrumental background since the start of the mission is shown in Fig.1 for CCD temperatures T>-55C and in the range -60C<T<-55C. The count rate is calculated for events collected outside the FoV and applying a 0 to 12 grade selection, merging the data for each month to obtain enough events. The plots show a very scattered and irregular background behavior over the monitored years which is likely due to "flickering pixels" producing high levels of dark current at intermittent times and to the background temperature dependence of individual data sets within the selected temperature range. However, the comparison of the count rate from early 2005 and the end of 2006 suggests no overall increase of the background level due to degradation of the CCD caused by interaction with high-energy particles.

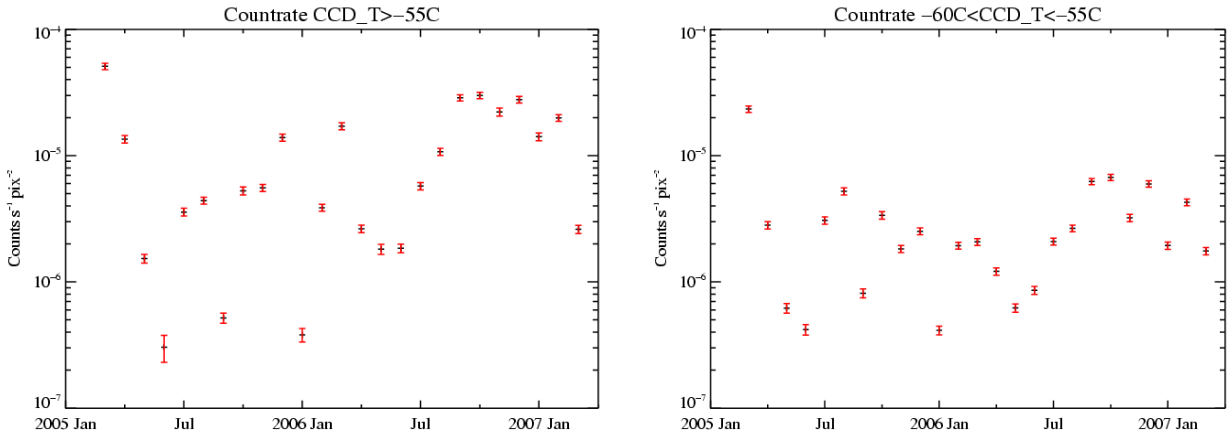

Fig. 1. Background count rate since the start of the mission at CCD temperatures T>-55C (left) and -60C<T<-55C (right). The count rate is lower at colder CCD temperatures. The comparison of early data points with count rates at later times does not indicate an overall increase in the background level.

In Fig. 2 we show the background spectra for the years 2005 and 2006, extracted by selecting grades 0 to 12 and excluding hot pixels, for the same temperature ranges described above. The spectra match well overall, although there is an excess of events below 0.5 keV in the 2006 data, suggesting an increase of the instrumental noise at low energies. The spectral lines at 5.9 keV and 6.5 keV are due to Mn K-α and Mn K-β emission from the ^{55}Fe corner sources, respectively, that are not completely masked out in the screening process.

To investigate the corner source count rate, we selected events in a narrow energy range around 5.9 keV. As expected, the intensity of the line is decreasing according to the 2.7-year half-life of ^{55}Fe, confirming the corner sources as the origin of the emission (Fig. 3). The other spectral features correspond to the Nickel K-α and K-β lines at 7.48 keV and 8.26 keV and are due to high-energy particles interacting with the camera body.

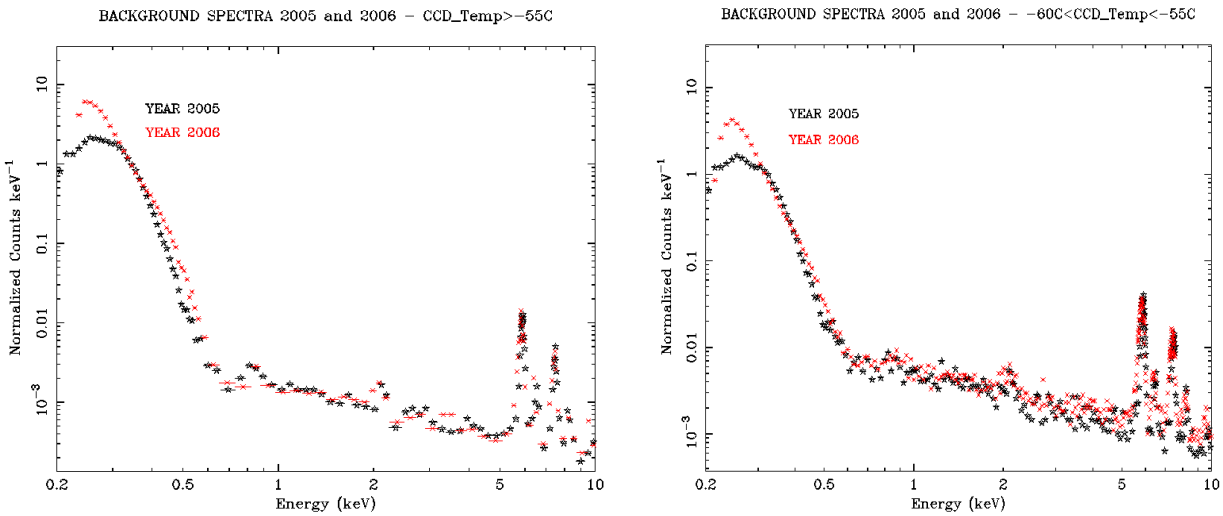

Fig. 2. Background spectra extracted at CCD temperature ranges of T>-55C (left) and -60C<T<-55C (right) from year 2005 and 2006. The spectra have been extracted by selecting event grades 0 to 12 only. For both temperature ranges, the comparison of the spectra shows an increase of low energy background events during 2006 compared to 2005.

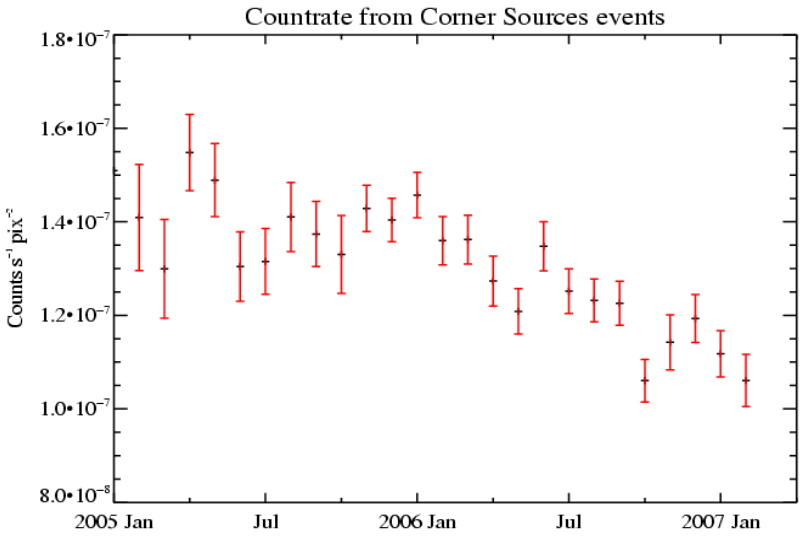

Fig. 3. The count rate of the events from the spectral line at 5.9keV has decreased since the start of the mission. These events are produced by K-α emission of the ^{55}Fe radioactive corner sources with a half-life of 2.7 years.

3.2 Background variations after SAA passes

In Fig. 4 we show the background count rate from events outside the FoV at increasing time intervals after the end of the SAA passes. For every temperature range, the background count rate within one minute after the SAA pass is higher than at later times, where it appears approximately constant. The increase in the count rate is due to the interaction of high-energy particles while *Swift* passes through the SAA.

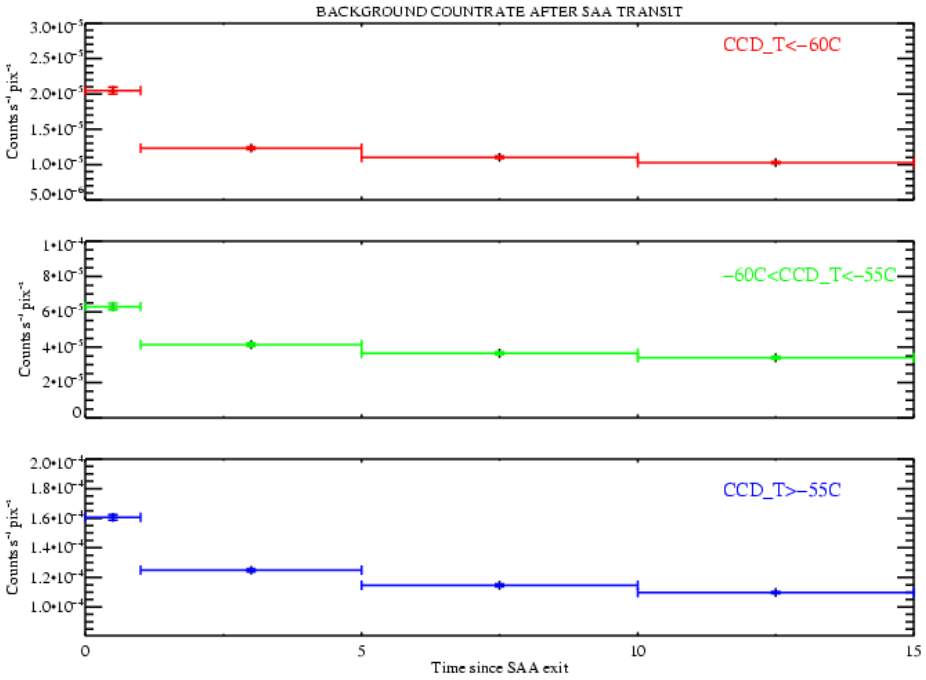

Fig. 4. The background count rate evaluated at increasing time intervals after the exit time of the SAA passes. The count rate is higher just after the SAA transit, and it levels off at later times.

The spectra of the merged event files at various time intervals after the SAA transits at *COLD* and *HOT* temperatures are shown in Fig. 5. The spectra have very similar shapes, both at higher and lower temperatures, and are dominated by the instrument noise. The lines at the high end of the spectra are due to corner sources events. There is no evidence for radioactive activation of the XRT by the SAA passes in these spectra.

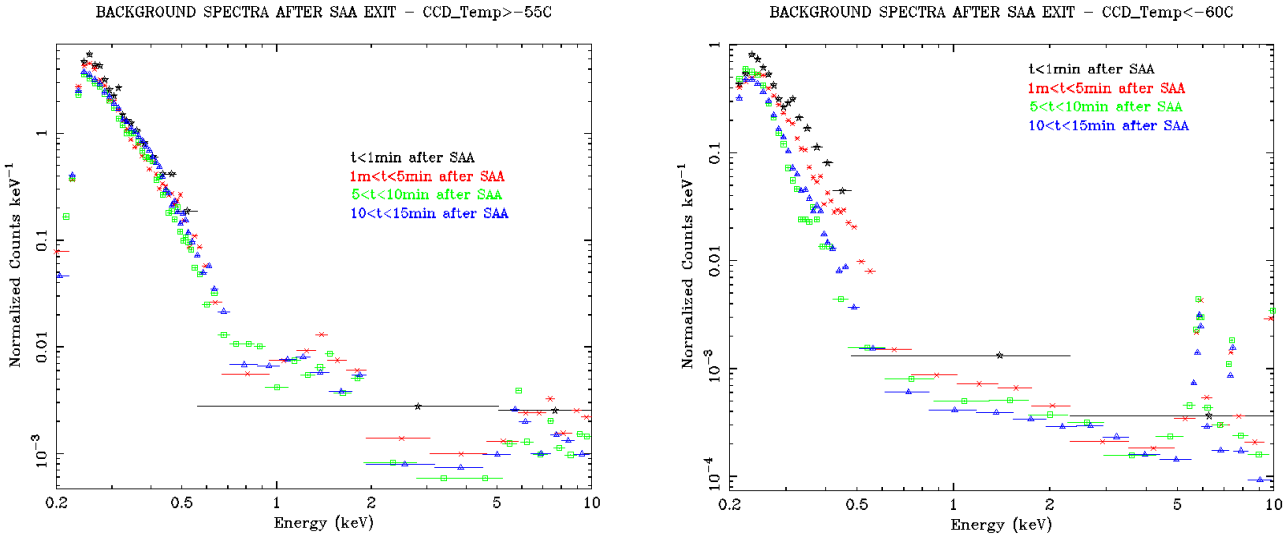

Fig. 5. The background spectra extracted at increasing time intervals after the exit time of the SAA passes for CCD temperatures T>-55C (left) and T<-60C (right).

3.3 Vignetting

In Fig. 6 we show the number of background events per pixel for the three previously defined temperature ranges in regions of increasing radii. The data were extracted in the 0.2 to 10.0 keV energy range. We fitted the measured counts as a function of the offset from the center of the chip with a linear combination of two components, a spatially constant component for the instrumental background and a second component with spatial dependence due to the vignetting effect (equation 1). At *HOT* temperatures, as expected, the fit is consistent with a spatially constant background, suggesting that the background is dominated by the noise of the detector. At *MEDIUM* and at *COLD* temperatures the best fit yields a vignetted component responsible for 28% and 10% of the measured background, respectively. The fit is shown as the straight line in Fig. 6. It is surprising that we found a larger cosmic X-ray background component at *MEDIUM* relative to *COLD* temperatures since we would expect the instrumental background component to decrease with temperature. This could be partially due to details of the algorithm used by the XRTPIPELINE to find and exclude bad and flickering pixels, a complex task due to the temperature variations of the CCD during long observations that modify the XRT background. This is especially evident at intermediate temperatures, just below -55C, when the number of hot pixels increases dramatically. This effect will be investigated in more detail in the future.

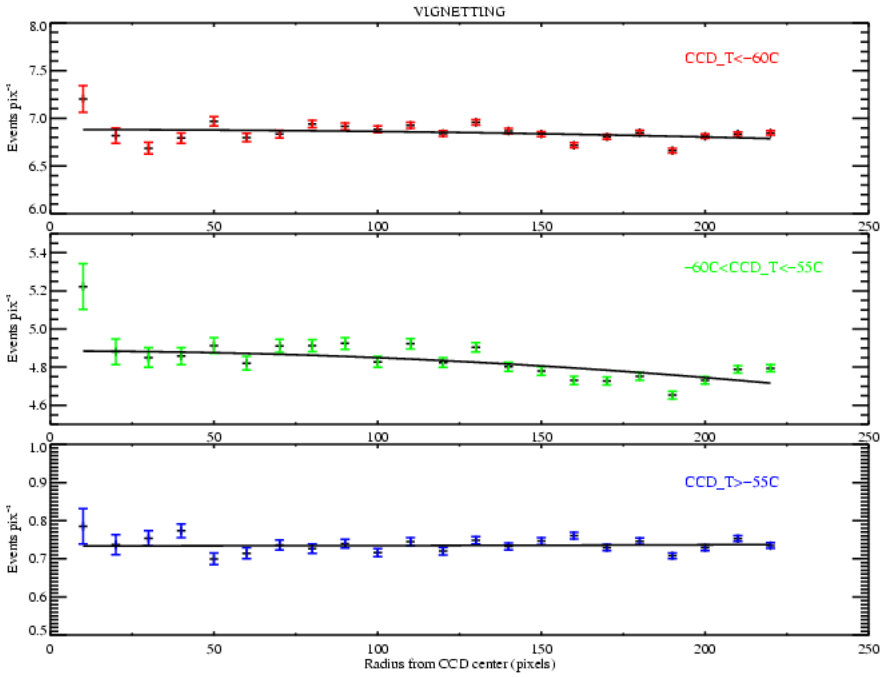

Fig. 6. Number of background events per pixel included in annular regions of increasing radii from the center of the chip at *COLD*, *MEDIUM* and *HOT* temperature ranges. The black lines are the best linear fit of the data with a constant component as the instrumental background and a vignetted component to account for the cosmic X-ray background.

The spectrum extracted from events collected outside the FoV for the analysis of the long-term background variation is purely instrumental background, while the spectrum extracted from events collected within the FoV, that we used for the vignetting analysis, is a combination of instrumental and unresolved X-ray cosmic background. In Fig. 7 we compare the two spectra, the spectrum extracted outside the FoV in red, the spectrum from events within the FoV in black.

The purely instrumental background spectrum presents a bump at low energies because for that analysis the XRTPIPELINE was not run on the datasets and the instrumental noise is not excluded. The spectral lines at high energy are from the corner sources events and from diffuse Nickel K-α and K-β events. The two spectra appear to have very similar shape at E>1 keV; we can infer that the observed spectra at these energies are dominated by the instrumental background, while the component from diffuse X-ray background becomes significant at energies between 0.5 and 1 keV.

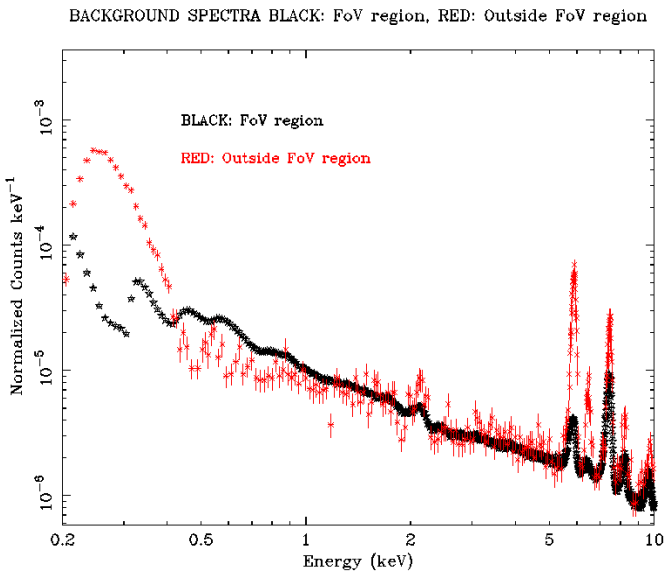

Fig. 7 Purely instrumental background spectrum extracted from events outside the FoV (in red) compared with background spectrum from events within the FoV, combination of instrumental background and unresolved diffuse cosmic X-ray background.

4. CONCLUSIONS

We analyzed *Swift* XRT archival data from 2005 and 2006 to study the evolution of the XRT background. The background time and spatial variations can be of primary importance for the study of extended sources such as supernova remnants or the analysis of the emission of the unresolved cosmic X-ray background.

Our analysis showed large variations of the XRT background during the mission, probably due to "flickering" pixels producing leakage current at intermittent times, nevertheless the comparison of the early 2005 and the late 2006 count rate does not show an overall increase in the background level. Our analysis of the purely instrumental background showed a short-term increase in the background count rate for time intervals within 1 minute after the SAA passes. We derived what fraction of the XRT background is purely instrumental and what part is due to diffuse cosmic background thanks to the knowledge of the functional form of the vignetting effect in XRT data. At T>-55C the background spectrum is consistent with a purely instrumental origin, while at colder temperatures the vignetted component constitutes up to 28% of the total background.

The *Swift* XRT team is planning a change of the substrate voltage (from 0 V to 6 V) to reduce the instrumental noise at low energies[14]. We will continue the present work on the XRT background to monitor its evolution with the raised substrate voltage.

5. ACKNOWLEDGEMENTS

This work is supported at Penn State by NASA contract NAS5-00136; at OAB by funding from ASI grant I/R/039/04; at the University of Leicester by the Particle Physics and Astronomy Research Council.

REFERENCES

1 D. N. Burrows *et al*., "The *Swift* X-ray Telescope", *Space Sci. Rev*., **120**, 165-195, 2005

2 S. Barthelmy *et al*., "The Burst Alert Telescope (BAT) on the *SWIFT* Midex Mission", *Space Sci. Rev*., **120**, 143-164, 2005

3 N. Gehrels *et al*., "The *Swift* Gamma-Ray Burst Mission", *ApJ*., **611**, 1005-1020, 2004
4 P. Romano *et al*., "*Swift*/XRT Observations of the Fifth Outburst of the Periodic Supergiant X-ray Transient IGR J11215-5952", *A&A*, **469**, L5, 2007
5 P. Brown *et al*., "Ultraviolet, Optical, and X-Ray Observations of the Type Ia Supernova 2005am with *Swift*", *ApJ*, **635**, 1192, 2005
6 D. Grupe *et al*,. "*Swift* Observations of the Highly X-ray Variable Narrow Line Seyfert Galaxy RX J0148.3-2758", *AJ*, **132**, 1189, 2006
7 O. Citterio *et al*., "Characteristics of the flight model optics for the JET-X telescope onboard the SPECTRUM X-γ satellite", *Proc. SPIE*, **2805**, 56-65, 1996
8 A. D. Holland, M. J. L. Turner, A. F. Abbey, P. J. Pool, "MOS CCDs for the EPIC on XMM", *Proc. SPIE*, **3445**, 13-27, 1998
9 A. F. Abbey *et al*., "Micrometeoroid damage to CCDs in XMM-Newton and *Swift* and its significance for future X-rays missions", Proceeding of the X-ray Universe Conference, El Escorial Spain, 2005 (see http://xmm.vilspa.esa.es/external/xmm_science/workshops/x-ray-symposium/175772_afa_micrometeoroids.pdf)
10 J. D. Carpenter *et al*., "Effects of micrometeoroid and space debris impacts in grazing incidence telescopes", *Proc. SPIE*, **6266**, 62633K, 2006
11 J. A. Kennea *et al*., "Controlling the *Swift* XRT CCD temperature via passive cooling", *Proc. SPIE*, **5898**, 589816-1, 2005
12 J. E. Hill *et al*., "Readout modes and automated operation of the *Swift* X-ray telescope", *Proc. SPIE*, **5165**, 217, 2004
13 Tagliaferri *et al*., "*Swift* XRT Effective Area measured at the Panter end-to-end tests", *Proc. SPIE*, **5165**, 241-250, 2004
14 J. Osborne *et al*., "The in-flight spectroscopic performance of the *Swift* XRT CCD camera", *Proc. SPIE*, **5898**, 352, 2005